Monthly Notices
of the
ROYAL ASTRONOMICAL SOCIETY

MNRAS **482,** 1872–1882 (2019)
Advance Access publication 2018 October 18

doi:10.1093/mnras/sty2805

Understanding WASP-12b

Avery Bailey★ and Jeremy Goodman
Department of Astrophysical Sciences, Princeton University, Princeton, NJ 08540, USA

Accepted 2018 October 15. Received 2018 October 14; in original form 2018 July 31

ABSTRACT

The orbital period of the hot Jupiter WASP-12b is apparently changing. We study whether this reflects orbital decay due to tidal dissipation in the star, or apsidal precession of a slightly eccentric orbit. In the latter case, a third body or other perturbation would be needed to sustain the eccentricity against tidal dissipation in the planet itself. We have analysed several such perturbative scenarios, but none is satisfactory. Most likely, therefore, the orbit really is decaying. If this is due to a dynamical tide, then WASP-12 should be a subgiant without a convective core as previous studies have suggested. We have modelled the star with the MESA code. Satisfactory main-sequence models can be found if the effective temperature is at the upper end of reported estimates, but subgiant models are in greater tension with current observational constraints.

Key words: planets and satellites: dynamical evolution and stability – planets and satellites: individual: WASP-12b – planet–star interactions – stars: individual: WASP-12.

1 INTRODUCTION

Much circumstantial evidence indicates that tidal dissipation sculpts the orbits of short-period binary stars and exoplanets. First principles tidal theories often have difficulty explaining the observations quantitatively, however. For example, among low-mass main-sequence binaries, the period below which orbits circularize appears to increase with system age up to periods $\sim$20 d, whereas standard dissipation mechanisms become ineffective beyond $\sim$10 d (Zahn 2013).

Transiting exoplanets offer the prospect of testing tidal dissipation in real time. Massive exoplanets with very short periods are expected to exhibit orbital decay due to tidal dissipation in their host stars, whose rotation is usually subsynchronous, on time-scales short compared to the star's main-sequence lifetime (Levrard, Winisdoerffer & Chabrier 2009). (This should not occur for stellar binaries because of the much greater angular momentum in the orbit, only a small fraction of which is needed to bring the stars into synchronous rotation.) In favourable cases where the inspiral time is $\lesssim 10^7$ yr, transit timing with subminute accuracy may be expected to detect the period change after a decade or so.

Currently the most promising tentative detection has been made for WASP-12b, a planet with mass $m_\mathrm{b} \approx 1.5\,M_\mathrm{J}$ in a 1.0914 d orbit around a main-sequence F star (Hebb et al. 2009). Highly statistically significant departures from a linear transit ephemeris have been measured by Maciejewski et al. (2016) and recently confirmed by Patra et al. (2017). According to the latter authors, the measured rate of change of orbital period is $\dot{P} = -29 \pm 3\,\mathrm{ms\,yr^{-1}}$, and $P/\dot{P} = 3.2\,\mathrm{Myr}$.

Three hypotheses for the orbital period change have been discussed. One is orbital decay. A second is precession of the periapse of a slightly eccentric orbit with a period $\sim$10 yr (Maciejewski et al. 2016). The required eccentricity is on the order of 10^{-3}, well below the limit $e < 0.05$ set by Husnoo et al. (2012). Patra et al. (2017) find that this explanation is disfavoured by times of planetary occultation (secondary eclipse) as measured with *Spitzer*: an eccentric orbit would tend to displace the times of primary and secondary eclipses in opposite directions, whereas the data seem to prefer an advance of both. Furthermore, it seems unlikely that even such a small eccentricity could have survived tidal dissipation in the planet. Nevertheless, Patra et al. (2017) conclude that apsidal precession cannot yet be definitively ruled out on the basis of the timing data.

The third possible explanation for $\dot{P}$ is acceleration by a companion. In fact WASP-12 is accompanied by a pair of M stars at projected separation $\approx$1 arcsec (Bechter et al. 2014). Given that the estimated mass of this pair is $\approx 0.75\,\mathrm{M_\odot}$ and the distance to WASP-12 is 432.5 ± 6.1 pc (Gaia Collaboration et al. 2018), the maximum line-of-sight acceleration is $\approx 0.33\,\mathrm{m\,s^{-1}\,yr^{-1}}$, corresponding to $|\dot{P}| < 0.1\,\mathrm{ms\,yr^{-1}}$, far smaller than the observed value. More to the point – because there might be unseen massive planets closer in – Knutson et al. (2014) have used their radial velocity data to place a limit $\lesssim 4\,\mathrm{m\,s^{-1}\,yr^{-1}}$ on this acceleration, and this is still almost an order of magnitude too small to explain $\dot{P}$.

In the absence of a plausible fourth hypothesis, orbital decay would therefore seem to be the best explanation for the observed departures from a linear ephemeris. There are, however, reasons for doubt. If the orbital decay time-scale is in fact only $\sim$3 Myr, whereas the main-sequence lifetime of the host star is $\gtrsim$1 Gyr (see Section 2), we must be viewing the system at a special time. On the other hand, WASP-12 is perhaps the best current candidate

★ E-mail: apbailey@princeton.edu

Table 1. Observed and adopted properties of WASP-12.

$T_{\rm eff}$ (K)	[Fe/H] (dex)	$\bar{\rho}$ ($\bar{\rho}_\odot$)	Reference
6300^{+200}_{-100}	$0.3^{0.05}_{0.15}$	0.35 ± 0.03	Hebb et al. (2009)
6250 ± 100	0.32 ± 0.12	–	Fossati et al. (2010b)
6118 ± 64	0.07 ± 0.07	–	Torres et al. (2012)
–	–	0.325 ± 0.016	Southworth (2012)
6313 ± 52	0.21 ± 0.04	–	Mortier et al. (2013)
–	–	0.315 ± 0.007	Maciejewski et al. (2013)
6241 ± 36	0.198 ± 0.032	0.3181 ± 0.0063	Adopted

for measurable orbital decay out of hundreds of hot Jupiters, so perhaps such a 'coincidence' should be less surprising. A potential concern is the small measured rotation: $v \sin i < 2.2\,{\rm km\,s^{-1}}$ (Hebb et al. 2009), $v \sin i < 5.1\,{\rm km\,s^{-1}}$ (Fossati et al. 2010b), or $v \sin i = 3.4 \pm 0.9\,{\rm km\,s^{-1}}$ (Torres et al. 2012). If the planetary orbit has donated much of its original angular momentum to the star, one might expect the star to have a larger $v \sin i$: the converse argument has been used by Penev et al. (2016) to suggest orbital decay in the HATS-18 system. In Sections 3 and 4.2, however, we demonstrate that this expectation is incorrect and that tidal mechanisms are insufficient to bring WASP-12 to full synchronous rotation. Instead, tidal mechanisms should spin-up only a small core region of the star – the observational effect of which we explore.

The orbital decay explanation has been previously investigated by Chernov, Ivanov & Papaloizou (2017) who determined that the observed decay could be sufficiently accounted for assuming that the dissipation is due to a fully damped dynamical tide. Though Chernov et al. (2017) make no investigation of whether the dynamical tide should be expected to be fully damped in the WASP-12 system, Weinberg et al. (2017) provide a plausible explanation for decay by offering the novel suggestion that WASP-12 is a subgiant. But because this particular system holds a unique and valuable place within the context of tidal theories and planet–star interaction, we felt it necessary to investigate this system further. We make a more thorough examination of stellar models before independently coming to similar interpretations as Weinberg et al. (2017). Our analysis also benefits from the most recent luminosity estimates for WASP-12 (see Section 2.3) and while the results are inconclusive, this new luminosity favours a higher mass main-sequence model. Bearing in mind this preference for a main-sequence model, we present a comprehensive investigation of alternative explanations for the observed period change in Section 5.

2 STELLAR MODELS

The tidal dissipation mechanisms discussed here are sensitive to the internal structure of the star, particularly the existence and extent of convection zones. Therefore, we begin by selecting a fiducial model for the WASP-12 host.

2.1 Properties of the WASP-12 star

Table 1 summarizes properties of WASP-12 as independently determined by the studies cited. The effective temperature and metallicity are in principle directly determinable by comparison of spectra with atmospheric models, while the mean stellar density $\bar{\rho} \equiv 3M_*/4\pi R_*^3$ follows from the orbital period and the fractional width R_*/a of the planetary transit. We have chosen not to use spectroscopic determinations of surface gravity, as some of these studies regard $\log g$ as problematic unless constrained by the mean density. The adopted values on the last line were obtained as a straightforward weighted average of the values shown:

$$\hat{X} = \hat{\sigma}^2 \sum_k \frac{X_k}{\sigma_k^2}, \qquad \hat{\sigma}^{-2} = \sum_k \frac{1}{\sigma_k^2}, \tag{1}$$

the original errors $\{\sigma_k\}$ being symmetrized where necessary, e.g. $6300^{+200}_{-100} \rightarrow 6300 \pm 150$. The adopted error $\hat{\sigma}$ is optimistic, especially for $T_{\rm eff}$ and [Fe/H], since the original errors are probably dominated by systematics of the atmospheric models.

2.2 Interior models

Models for WASP-12 were constructed using the 10 108 release of the publicly available 1D stellar evolution code MESA (Paxton et al. 2011, 2013, 2015, 2018). This version of MESA includes an improved prescription for determining radiative–convective boundaries, the locations of which can sensitively alter the strength of tidal effects. We arrived at a fiducial model for WASP-12 after searching the parameter space over mass M_* and initial metallicity $Z_{\rm init}$ with bounds $1.15 < M_* < 1.4\,{\rm M}_\odot$ and $0.01 < Z_{\rm init} < 0.033$. An unweighted sum of χ^2 statistics of the adopted properties listed in Table 1 was chosen as the goodness-of-fit statistic to be minimized over the searched parameter space. Though we conducted searches including all three observables in the goodness-of-fit statistic $\chi^2\,(\bar{\rho}, T_{\rm eff}, {\rm [Fe/H]})$, here we focus on the results of searches for the statistic $\chi^2\,(\bar{\rho}, T_{\rm eff})$ that omit [Fe/H]. Both statistics give similar results, but the latter lends itself to analysing the observables in an individual sense instead of a combined one. For our calculation of the model $[{\rm Fe/H}] \equiv \log_{10}(Z_{\rm surf}/X_{\rm surf}) - \log_{10}({\rm Z}_\odot/{\rm X}_\odot)$, we adopted the Asplund et al. (2009) value, ${\rm Z}_\odot/{\rm X}_\odot = 0.0181$. For each combination of M_* and $Z_{\rm init}$, a stellar model was evolved from pre-main sequence with our goodness-of-fit statistic evaluated at each time step until the statistic moved far enough from a local minimum to trigger the stopping conditions for that evolutionary run.

For all parameter space searches we adopted the physics of Choi et al. (2016), but tested two mixing length parameter values of $\alpha = 1.9$ and 2.3. The results of a series of evolutionary runs according to both several grids and simplex searches for $\chi^2\,(\bar{\rho}, T_{\rm eff})$ are displayed in Fig. 1 for $\alpha = 1.9$ and in Fig. 2 for $\alpha = 2.3$. We highlight three models in particular between Figs 1 and 2 and provide additional details in Table 2. The first model, model A, is representative of a class of models that are on the main-sequence, plus are able to adequately fit the observed $\bar{\rho}$, $T_{\rm eff}$, and [Fe/H]. Most significantly, models of this type have a small convective core. If WASP-12 had no convective core, gravity waves excited at the outer convective–radiative boundary might deposit their angular momentum by breaking non-linearly at the inner turning point where the Brunt–Väisälä N equals the tidal frequency ω (Goodman & Dickson 1998; Terquem et al. 1998; Barker & Ogilvie 2010; Weinberg et al. 2017). The convective core in these models removes the possibility of this dissipation mechanism by moving the turning point outward to a region where the gravity waves lack the amplitude to break. As we show in Sections 3 and 4.1, models with the structure of model A are unable to explain the observed tidal decay of WASP-12b.

This motivated the search for an additional class of models that lack a convective core. At lower masses, the convective core of models that still fit the observed $\bar{\rho}$ and $T_{\rm eff}$ shrinks. This continues until, as is displayed in Figs 1 and 2, the convective core disappears entirely around a mass of $\approx 1.2\,{\rm M}_\odot$ where the well-fitting models become subgiants. We focus on two representative subgiant models that we refer to as models B and C, differentiated by having $\alpha = 1.9$

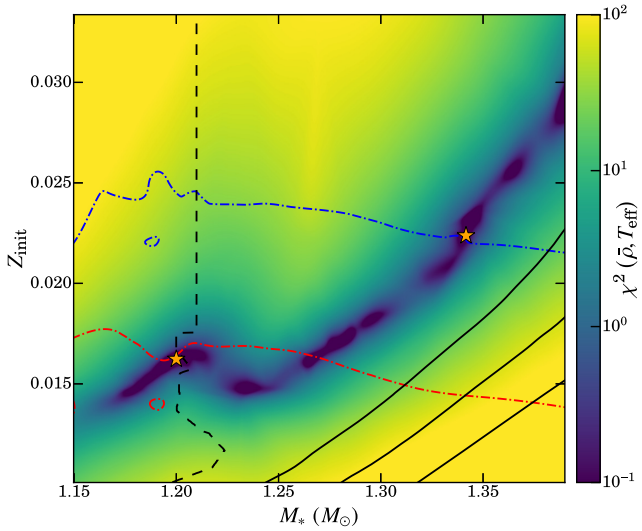

Figure 1. The tested parameter space over initial mass and metallicity coloured according to the goodness-of-fit statistic under a cubic interpolation. The dot–dashed lines are contours for [Fe/H] with the higher metallicity blue line marking our fiducial value and the lower metallicity red line marking the solar value. Solid black contours for luminosity are placed at the level $\log_{10}(L_*/\mathrm{L}_\odot) = 0.65$ with ±10 per cent error bars. Models with masses lower than the black dashed line have a radiative core, whereas higher masses have a small convective core. These models assume mixing length parameter $\alpha = 1.9$. The location of models A and B are marked with stars.

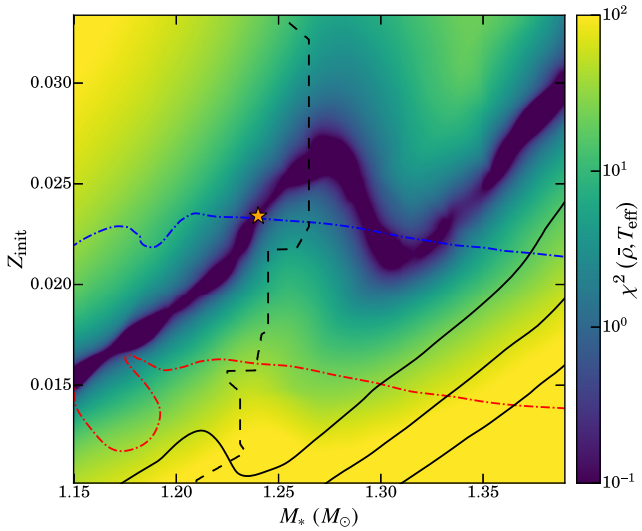

Figure 2. The tested parameter space for models with mixing length parameter $\alpha = 2.3$. Plotted according to the caption in Fig. 1 with the location of model C marked with a star.

and 2.3, respectively. Unfortunately, each of these models suffers from inconsistencies: model B having too low surface metallicity to match observations and model C having an uncomfortably large α (see below).

Although our fiducial value for the error on [Fe/H] is undoubtedly optimistic, past analyses have all concurred that WASP-12 has supersolar surface abundance, whereas our model B is near solar or slightly subsolar. As the surface metallicity is dependent upon the prescription for elemental diffusion and stellar rotation, we also tested an alternative prescription more tailored to WASP-12 than Choi et al. (2016), assuming a rotation rate of $\approx$10 km s^{-1}. This rotation rate was informed by measurements of the Rossiter–McLaughlin effect in this system that indicate a strong spin–orbit misalignment of $59^{+15}_{-20}{}^\circ$ and that $v \sin i_* = 1.6^{+0.8}_{-0.4}$ km s^{-1} (Albrecht et al. 2012). Corresponding changes to the surface metallicity were minimal and it seems unlikely that any rotation or diffusion mechanism would be able to significantly enhance the surface metallicity above $Z_{\rm init}$ to reproduce the observed [Fe/H].

Though model C fits well for all three observables, it assumes $\alpha = 2.3$, in what is probably an unrealistically high choice of α. As Procyon is a spectral neighbour to WASP-12 and is particularly well constrained, it provides reasonable calibration for α. Assuming a mass of $1.478 \pm 0.012\,\mathrm{M}_\odot$ (Bond et al. 2015), setting initial [Fe/H] equal to the observed [Fe/H] $= -0.05 \pm 0.03$ (Allende Prieto et al. 2002), models with $\alpha \geq 2.2$ cannot simultaneously reproduce the observed $T_{\rm eff} = 6516 \pm 87$ K (Aufdenberg, Ludwig & Kervella 2005), luminosity $\log_{10}(L/\mathrm{L}_\odot) = 0.84 \pm 0.018$ (Jerzykiewicz & Molenda-Zakowicz 2000), and $\bar{\rho} = 0.1725 \pm 0.0007\,\rho_\odot$ (Bedding et al. 2010). Instead, the best-fitting models occur in the range $1.8 \leq \alpha \leq 2.1$. Solar calibrations corroborate this suggesting $\alpha = 1.93$ (van Saders & Pinsonneault 2012), $\alpha = 1.82$ (Choi et al. 2016), etc.

Although we certainly have not exhausted the parameter space of possible subgiant models, and there are enough tuneable parameters in stellar modelling that it may be possible to construct a subgiant model that fits the observables, with standard assumptions it is difficult to do so. On the other hand, main-sequence models that fit the observables (except the luminosity – see below) are generic and easy to find, which is likely why previous studies estimate the mass of WASP-12 to be near 1.4 $\mathrm{M}_\odot$ (Southworth 2012; Collins, Kielkopf & Stassun 2017). Though the convective core in these models inhibits tidal decay via breaking of gravity waves, the presence of a convective envelope allows for damping of the equilibrium tide (Section 3) and dynamical tide (Section 4.1) by turbulent viscosity (Zahn 1977). In these later sections, however, we adopt model A as a fiducial model to show that both the equilibrium tide and dynamical tide in main-sequence models are unable to explain WASP-12b's decay.

2.3 WASP-12 luminosity

In addition to using $\bar{\rho}$ and $T_{\rm eff}$ to constrain stellar models, we made some investigation of whether our models A, B, and C could be constrained via luminosity measurements. The most recent parallax measurements made by the *Gaia* mission (Gaia Collaboration et al. 2016, 2018) place WASP-12 at a distance of 432.5 ± 6.1 pc, significantly further than past determinations. Adapting the work of Stassun, Collins & Gaudi (2017), who estimate the extinction to WASP-12 at $A_V = 0.29$ mag, to this updated distance measurement gives a luminosity of $\log_{10}(L_*/\mathrm{L}_\odot) = 0.65$. Taking L_* together with our selected values of $T_{\rm eff}$ and $\bar{\rho}$ uniquely determines the mass at $M_* \approx 1.9\,\mathrm{M}_\odot$. Such a high mass would seem to favour the higher mass main-sequence models for WASP-12 but evolutionary runs at $1.9\,\mathrm{M}_\odot$ fail to simultaneously fit these three observables. Figs 1 and 2 similarly suggest that any model significantly larger than $1.4\,\mathrm{M}_\odot$ and having the requisite $T_{\rm eff}$, $\bar{\rho}$ would require an unrealistically high metallicity. For example, even the best-fitting highest metallicity $1.9\,\mathrm{M}_\odot$ model tested ([Fe/H] ≈ 0.4) had a value $\chi^2(\bar{\rho}, T_{\rm eff}, L_*) > 100$. The incompatibility of these three observables is also visible in Figs 1 and 2 as lines of constant L_* lie parallel to the track of constant $\bar{\rho}$, $T_{\rm eff}$. This tension between measured ob-

Table 2. Fiducial WASP-12 models.

Name	α	$Z_{\rm init}$	M_* ($M_\odot$)	Age (Gyr)	$\log_{10}(L_*/L_\odot)$	$T_{\rm eff}$ (K)	[Fe/H] (dex)	$\bar{\rho}$ ($\bar{\rho}_\odot$)	$\chi^2(\bar{\rho}, T_{\rm eff})$	χ^2([Fe/H])
A	1.9	0.0223	1.34	2.72	0.55	6250	0.20	0.3182	0.064	0.031
B	1.9	0.0162	1.20	4.24	0.52	6242	−0.03	0.3185	0.006	49.06
C	2.3	0.0234	1.24	4.51	0.53	6245	0.20	0.3181	0.017	0.006

servables is alleviated as one goes to either higher $T_{\rm eff}$ or lower luminosity.

While *Gaia* Data Release 2 (DR2) lists a very precise parallax for WASP-12, 2.3122 ± 0.0325 mas, the extinction (A_G) is not reported. Without correction for extinction, the reported luminosity is $3.435 \pm 0.075\,L_\odot$, which is entirely compatible with the models in Table 2. One might therefore worry that Stassun et al. (2017) have overestimated the extinction or the flux – the former perhaps because some of the photometric data they used were published before it was recognized that the star has two M-dwarf companions within 1 arcsec (Bergfors et al. 2013). But for comparison, the dust map of Green et al. (2018)[1] predicts $E(B-V) = 0.07^{0.02}_{0.03}$ mag at 440 pc in the direction of WASP-12, which would correspond to $A_V \approx 0.21 \pm 0.09$ mag for a normal extinction curve. Querying the *Gaia* DR2 catalogue for stars within 1° of WASP-12, parallaxes $\geq$2.28 mas, and $T_{\rm eff} > 5500$ K yields 101 results, of which 78 have A_G values listed. There is no clear trend with distance, but the median A_G for the more distant half of this sample is 0.23 mag. These are slightly lower than the Stassun et al. (2017) estimate, but consistent within the uncertainties. So it seems that WASP-12 is at least ∼10–30 per cent more luminous than any of the models in Table 2.

Considering these three independently determined observables ($\bar{\rho}$, $T_{\rm eff}$, L_*) are incompatible with one another, we also ran a chi-square model search including the luminosity, with 10 per cent errors on L_*. As one can infer from inspection of the luminosity contours in Figs 1 and 2, including L_* in the search moves the track of well-fitting models towards lower metallicity such that it lies between the low $\chi^2(\bar{\rho}, T_{\rm eff})$ track and the $\log_{10}(L_*/L_\odot) = 0.65$ contour. As the three observables are incompatible, $\chi^2(\bar{\rho}, T_{\rm eff}, L_*)$ becomes significantly larger, with minimum $\chi^2 \approx$ 3–5, depending on α and assuming 10 per cent error bars on the luminosity. Ultimately, it seems that because lines of constant $\bar{\rho}$, $T_{\rm eff}$ lie nearly parallel to lines of constant L_* in the $Z_{\rm init}-M_*$ plane that luminosity measurements offer little guidance in choosing between models of type A, B, or C (at least in the mass range $1.15 < M_* < 1.4\,M_\odot$ and under our fiducial values for $T_{\rm eff}$ and $\bar{\rho}$).

Though the observables ($\bar{\rho}$, $T_{\rm eff}$, L_*) are incompatible under our assumed fiducial values of $T_{\rm eff}$ and $\bar{\rho}$, a higher assumed effective temperature for WASP-12 can alleviate this tension entirely. In Fig. 3 we display the results of a χ^2 search ($\alpha = 1.9$) adopting a higher temperature $T_{\rm eff} = 6360 \pm 130$ K and $\bar{\rho} = .3164 \pm .0106\,\rho_\odot$ from Collins et al. (2017).[2] With the higher temperature of 6360 K, best-fitting models are starting to match the *Gaia* DR2 luminosity with reasonable values of M_* and $Z_{\rm init}$. The most compatible models lie in the mass range $1.4 \lesssim M_* \lesssim 1.6$, have significantly supersolar metallicities, and are main-sequence models [the very highest mass and metallicity models being zero-age main sequence (ZAMS)]. Fig. 3 may hint at a preference for main-sequence models

[1]Which can be queried at `argonaut.skymaps.info`

[2]The Collins et al. (2017) adopted temperature is actually 6360^{+130}_{-140} K and though we use their $\bar{\rho}$ it is consistent with our own fiducial estimate for $\bar{\rho}$.

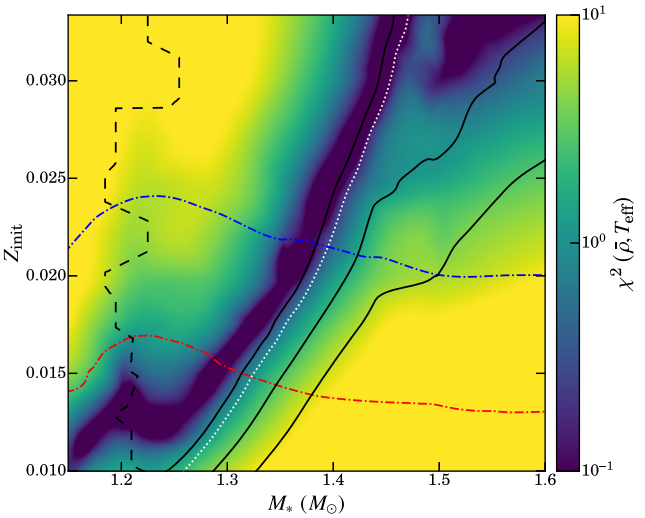

Figure 3. A set of models with mixing length parameter $\alpha = 1.9$, but fitting for a hotter $T_{\rm eff} = 6360 \pm 130$ K. Plotted according to the caption in Fig. 1, but note that this parameter space extends to higher M_* and that the colourmap has been rescaled because the uncertainties adopted in this χ^2 search were significantly larger. The branch of well-fitting models with the very highest masses and metallicities is ZAMS. An additional dotted white luminosity contour has been placed at the level of the *Gaia* luminosity assuming an −80 μas offset to the parallax (see text).

over the subgiant ones because the subgiant models have subsolar [Fe/H] and seem to lie further from the *Gaia* DR2 luminosity contours, but the uncertainties on the adopted $T_{\rm eff}$ are too large to make any conclusive statements. A lower luminosity could also play a role to relieve the tension (though to a lesser extent than $T_{\rm eff}$ it seems). To illustrate this point, in Fig. 3 we include a contour for a correction to our luminosity assuming a −80 μas systematic offset *Gaia* DR2 parallaxes argued for by Stassun & Torres (2018).

On the other hand, if a significantly lower temperature than our fiducial value is assumed, the discrepancy between observables grows. We carried out a similar analysis to the high temperature treatment above, but using the low temperature $T_{\rm eff} = 6118 \pm 64$ given by Torres et al. (2012). We do not display the results here because we find all low temperature models more discrepant with L_* than the equivalent models shown in Fig. 1. For the purposes of stellar modelling, past determinations of $T_{\rm eff}$ that have erred on the hot side are significantly preferred.

3 EQUILIBRIUM TIDE

The adiabatic equilibrium tide describes the hydrostatic tidal response of the host star to a perturbing body in the absence of dissipation. In this hydrostatic limit where the tidal frequency ω goes to zero, the functional relationship between density ρ, pressure p, and total gravitational potential (including that of the perturbing companion) Φ is preserved. As a result, density and pressure are

constant along equipotentials and have the same value on a given equipotential as they would on the same equipotential absent the tide. If one neglects composition gradients, entropy S is a function of ρ and P only and would consequently follow the equipotentials. In regions with a non-zero entropy gradient, i.e. radiative zones, the adiabatic condition would require fluid elements also stay tied to equipotentials ($\xi_r^{\rm eq} \propto \Phi_1$, the subscript 1 indicating an Eulerian perturbation). The equilibrium tide is also incompressible, $\nabla \cdot \boldsymbol{\xi}^{\rm eq} = 0$. In stably stratified regions the radial fluid displacement is explicitly described by the equation

$$\xi_r^{\rm eq} = \frac{\Phi_1}{{\rm d}\Phi/{\rm d}r}. \tag{2}$$

With the addition of composition gradients, though the above entropy argument no longer holds, a similar result can be derived (Goodman & Dickson 1998; Terquem et al. 1998). Namely, the fluid displacements are still described by equation (2) and are still incompressible where the squared Brunt–Väisälä frequency $N^2 \neq 0$. In convective regions where the entropy gradient vanishes, and $N^2 = 0$, fluid displacements may not necessarily follow the above equation (2) but one defines the equilibrium tide such that equation (2) is satisfied.

In convective regions of a star, turbulent viscous forces facilitate the cascading of bulk kinetic energy to smaller scales where it is dissipated. The form of this dissipative system and its action on the equilibrium tide in stars with a convective region was developed by Zahn (1966) and dissipates the energy on a time-scale (Remus, Mathis & Zahn 2012)

$$\frac{1}{t_{\rm diss}} = 4\pi \frac{6264}{35} \frac{R_*}{M_*} \int_{R_+/R_*}^{1} \rho \nu_{\rm t} x^8 {\rm d}x, \tag{3}$$

where $x \equiv r/R_*$ is the fractional radius, R_+ is the radius of the outermost radiative–convective boundary, and $\nu_{\rm t}$ is the convective viscosity. Here we have restricted the limits of integration to extend only over the convective envelope as the equivalent contribution due to the convective core is heavily suppressed by the x^8 dependence within the integrand. Equation (3) operates under the assumption of a thin convective envelope. Stated more precisely:

(i) the mass of the convective region is negligible ($M_* \approx M_+$);
(ii) the self-interacting perturbation to the potential caused by equilibrium tide displacements $\Phi_{1,*}$ is small compared to the perturbation to the potential caused by the star's external companion $\Phi_{1,{\rm b}}$ ($\Phi_{1,*} + \Phi_{1,{\rm b}} \approx \Phi_{1,{\rm b}}$);
(iii) the stellar invariant U is small compared to unity ($U \equiv {\rm d}\ln M/{\rm d}\ln R \ll 1$).

Our fiducial WASP-12 models satisfy the above criteria for a thin convective envelope with the convective envelope containing $<$ 0.2 per cent of the mass of the star, $\Phi_{1,*} < 0.03\Phi_{1,{\rm b}}$, and the stellar invariant $U < 0.025$.

In calculating the dissipation rate associated with the equilibrium tide, we assume a viscosity of the form

$$\nu_{\rm t} = \frac{l_{\rm c} u_{\rm c}}{\sqrt{1 + (\tau_{\rm c}/P_{\rm tide})^{2\beta}}}, \tag{4}$$

where $l_{\rm c}$ is the mixing length, $u_{\rm c}$ is the rms vertical convective velocity, $\tau_{\rm c} \equiv 2l_{\rm c}/u_{\rm c}$ is twice the local convective turnover time and $P_{\rm tide} = 2\pi/\omega$ is the tidal period. When $\beta = 1$, this form of the viscosity is a heuristic that reproduces the turbulent viscosity formalism of Zahn (1966) in the limit that $P_{\rm tide} \gg \tau_{\rm c}$ and $P_{\rm tide} \ll \tau_{\rm c}$. The suppression of viscosity that arises in Zahn's formalism for $P_{\rm tide} \ll \tau_{\rm c}$ comes from the fact that for large tidal frequencies, eddies are unable to travel a full mixing length. One then supposes that the mean free path of such an eddy should be replaced by the distance an eddy travels in something like half a tidal period, resulting in a suppression by a factor of $P_{\rm tide}/\tau_{\rm c}$. Others such as Goldreich & Nicholson (1977) have argued that eddies with turnover times greater than the tidal period do not 'exchange momentum with the mean flow on this time-scale [the tidal period]' and therefore do not contribute to the turbulent viscosity. The result is a suppression of the viscosity that is quadratic in $P_{\rm tide}/\tau_{\rm c}$ rather than linear ($\beta = 2$). Simulations done by Penev et al. (2007) recover a suppression in the vertical component of the viscosity that scales almost linearly, whereas the simulations of Ogilvie & Lesur (2012) indicate a quadratic suppression in the high-frequency regime. This uncertainty in the form of the viscosity remains an outstanding problem in tidal theory, but in the values that follow we have assumed Zahn's formalism ($\beta = 1$) so as to maximize the dissipation.

Taking radial profiles for the mixing length and convective velocity from our fiducial models of WASP-12, assuming Zahn's scaling of the viscosity, and integrating over the convective envelope yields $t_{\rm diss} \approx 300$ yr. From the rate of dissipation, an estimate for the orbital semimajor axis $a \approx 0.0234$ au and the stellar moment of inertia I_*, one can also estimate the synchronization time (Zahn 2013)

$$\frac{1}{t_{\rm sync}} = \frac{1}{t_{\rm diss}} \frac{m_{\rm b}^2 R_*^2}{M_* I_*} \left(\frac{R_*}{a}\right)^6, \tag{5}$$

which yields $t_{\rm sync} \approx 11$ Gyr. This suggests that viscous dissipation of the equilibrium tide is too weak to have significantly spun-up the star, a result consistent with observations assuming a low initial rotation rate. The corresponding orbital decay rate however,

$$\frac{P}{\dot{P}} = \left(\frac{m_{\rm b} a^2}{2I_*}\right) t_{\rm sync} \approx 1.2\,{\rm Gyr}, \tag{6}$$

is several orders of magnitude too long to explain the observed decay.

4 DYNAMICAL TIDE

In addition to the hydrostatic tidal response of the equilibrium tide, there must also exist a low-frequency dynamical response that mathematically arises from a condition for the continuity of fluid displacements across the radiative–convective boundary of the star. Dubbed the dynamical tide, this fluid response results in the excitation of internal gravity waves at the star's radiative–convective boundary that propagate inwards to be damped by radiative diffusion. The dynamical tide couples to the star's natural eigenfrequencies, potentially dissipating the tide at a rate orders of magnitude above the equilibrium rate if the system lies close to resonance. Provided the damping mechanisms acting on the dynamical tide are efficient to the point where waves are being damped before returning to the radiative–convective boundary, the resonances are broadened to the point of overlap. Under the assumption that the resonances overlap, the dissipation rate is estimated as a frequency average over the resonances. Adapting an expression for the frequency-averaged torque $\bar{\tau}$ from Kushnir et al. (2017) to WASP-12's outer convective boundary and using quantities obtained from our fiducial models:

$$\bar{\tau} \approx \frac{G m_{\rm b}^2}{R_+} \left(\frac{R_+}{a}\right)^6 \left(\frac{R_+^3}{G M_+}\right)^{4/3} \frac{\rho_+}{\bar{\rho}_+} \left(1 - \frac{\rho_+}{\bar{\rho}_+}\right)^2 \omega^{8/3}$$
$$\approx 3 \times 10^{-7} \left(\frac{G m_{\rm b}^2}{a}\right), \tag{7}$$

where ρ_+ is the mass density at R_+, $\bar{\rho}_+$ is the mean mass density interior to R_+, and M_+ is the mass interior to R_+. Though there is an analogous torque caused by waves excited at the inner radiative–convective boundary for model A, the frequency averaged torque is some eight orders of magnitude smaller as $\bar{\tau} \propto r^9$. The circular orbital decay rate corresponding to the above torque is

$$\frac{\dot{a}}{a} = -\frac{2\bar{\tau}}{m_{\rm b}\sqrt{GM_* a}} \approx -\frac{1}{1\,{\rm Myr}}, \tag{8}$$

which is fairly close to the observationally inferred decay rate $\dot{a}/a = (4.8\,{\rm Myr})^{-1}$, especially in view of the uncertain depth of the thin convection zone and consequent uncertainty of ρ_+ above. This picture of tidal decay via the dynamical tide is a natural explanation for any models with a radiative core such as B and C. Tidally excited internal gravity waves would freely propagate inwards and break near the centre of the star, resulting in the above decay rate. But as these models have their drawbacks (see Section 2), we now ask whether models with a convective core such as model A have a mechanism to recover the frequency-averaged torque.

4.1 Damping rates

The frequency-averaged torque can be recovered by model A if the radiative diffusion time-scale or the viscous damping time-scale in the convective envelope is comparable to the propagation time for a gravity wave. Because the Kelvin–Helmholtz time-scale in roughly solar-mass stars is relatively long, we operate under a quasi-adiabatic assumption in calculating these damping rates. The relevant linearized work integral for calculating the radiative diffusion time-scale is

$$W \approx -\int_{R_-}^{R_+} \frac{\delta T}{T} \left(\nabla \cdot \boldsymbol{F}_1\right) {\rm d}^3\boldsymbol{r}, \tag{9}$$

where δT is the Lagrangian perturbation to temperature and the Lagrangian heat flux perturbation $\delta \boldsymbol{F}$ is replaced with $\boldsymbol{F}_1$, its Eulerian perturbation, because the star is approximately in nuclear equilibrium on time-scales short compared to the main-sequence lifetime. We allow the integral to range from the inner radiative–convective boundary (R_-) to the outer one (R_+) rather than the whole of the star. Though there is a small positive contribution to the work integral from the convective regions, the contribution is small because the work integral ends up being proportional to the superadiabatic gradient $(\nabla_{\rm ad} - \nabla) \ll 1$. Because the wavelength of these modes is small compared to a pressure scale height H_p, the opacity can be approximated as roughly constant and the above integral simplifies to

$$W \approx \int_{R_-}^{R_+} KT\nabla_{\rm ad}\left(\nabla_{\rm ad} - \nabla\right)\left[\left|\frac{{\rm d}\xi_r}{{\rm d}r}\right|^2 + \frac{l(l+1)}{r^2}\left|\xi_r\right|^2\right]{\rm d}r, \tag{10}$$

where l is a mode's angular order, K is the thermal conductivity, ∇ is the temperature gradient, and $\nabla_{\rm ad}$ is the adiabatic temperature gradient. To determine the linear eigenfunctions ξ_r, ξ_h we numerically integrated the well-known fourth-order set of stellar structure equations for linear, adiabatic, non-radial perturbations by shooting to a fitting point at the outer radiative–convective boundary. This yielded a radiative damping rate $\gamma_{\rm rad} \approx (300\,{\rm yr})^{-1}$. Because this is orders of magnitude slower than the propagation time,

$$t_{\rm prop} = \int \left|\frac{\partial k_r}{\partial \omega}\right| {\rm d}r \approx \frac{\sqrt{l(l+1)}}{\omega^2}\int_{R_-}^{R_+} \frac{N}{r}{\rm d}r \approx 9\,{\rm d}, \tag{11}$$

radiative diffusion by itself is not significant enough to broaden the resonant peaks to the point of overlap.

Although convective viscosity is not effective at dissipating the equilibrium tide in this system, convective viscosity could also damp internal gravity waves as they evanesce in convective regions. The total viscous diffusion associated with shear tensor σ_{ij} and dynamic viscosity μ in Einstein notation is

$$\dot{E}_{\rm visc} = \int \mu\left(\sigma_{ij}^2 - \frac{1}{3}\sigma_{ii}^2\right){\rm d}^3\boldsymbol{r} \approx \int \mu\sigma_{ij}^2 {\rm d}^3\boldsymbol{r}. \tag{12}$$

Solving for the squared components of the shear tensor in spherical polar coordinates, we find that the viscous work due to convection is of the form

$$\dot{E}_{\rm visc} = \omega^2 \int r^2{\rm d}r\mu\left[\left|\frac{{\rm d}\xi_r}{{\rm d}r}\right|^2 + 2\left(l^2+l+1\right)r^{-2}\left|\xi_r\right|^2 - 5l(l+1)r^{-2}\Re\left(\xi_h^*\xi_r\right) + l(l+1)(l^2+l+1)r^{-2}\left|\xi_h\right|^2\right]. \tag{13}$$

For model A, this work integral corresponds to a damping rate of $\gamma_{\rm visc} \approx (300\ {\rm yr})^{-1}$, still substantially long to inhibit averaging over the resonances. As with the equilibrium tide, this estimate has assumed a linear scaling in the viscosity ($\beta = 1$) to maximize the dissipation.

Though we cannot justify the use of a frequency-averaged dissipation to explain the observed decay, it's possible that we are observing this system sufficiently close to resonance to produce a high decay rate. Adopting a damping rate, $1/\gamma \equiv 1/\gamma_{\rm rad} + 1/\gamma_{\rm visc}$, a circular orbit (consistent with observations) and uniform observation in time, the probability of seeing the system with observed decay rate with its 1σ errors, $-32 < \dot{P} < -26\,{\rm ms\,yr^{-1}}$, is at the level of $\approx 10^{-7}$. Of course this probability should not be accepted in a rigorous sense because it ignores selection biases, but it is still instructive to share how truly little the resonances are broadened by our selected damping mechanisms.

Without an effective damping mechanism, it is still possible to recover a frequency-averaged decay rate if the modes excited in the star are able to overturn stratification and break at some radius in their zone of propagation, thus depositing all their energy. In regions of the star where $N^2 \propto r$, the linear criterion for breaking is simply $\Delta \equiv r^{-1}\partial_r\left(r\xi_r\right) > 1$. Fig. 4 shows the maximal value of Δ in models A and B for a range of orbital periods. Because $\Delta_{\rm max} > 1$ only for ω close to resonance, wave breaking in model A does not provide a natural explanation for the tidal decay. However, for models such as B and C that lack a convective core, the inner turning point is so close to the centre that the condition for wave breaking there is marginally satisfied even in the valleys between resonances.

4.2 Rotational effects

Assuming that WASP-12b's signature is indeed due to decay via the dynamical tide, as is suspected for model B or C, the extent to which the star should have been spun-up to synchronous rotation can be explicitly calculated. Even though WASP-12 is observed to have small surface rotation, at least some part of the core of the star should have been spun-up from internal gravity waves breaking and depositing their angular momentum. We make the approximation that the relevant torque is changed appreciably only by changes to the orbit and not by changes to the star itself, so that $\tau \propto a^\eta$. Given the period of time that the dynamical tide has been acting Δt, the

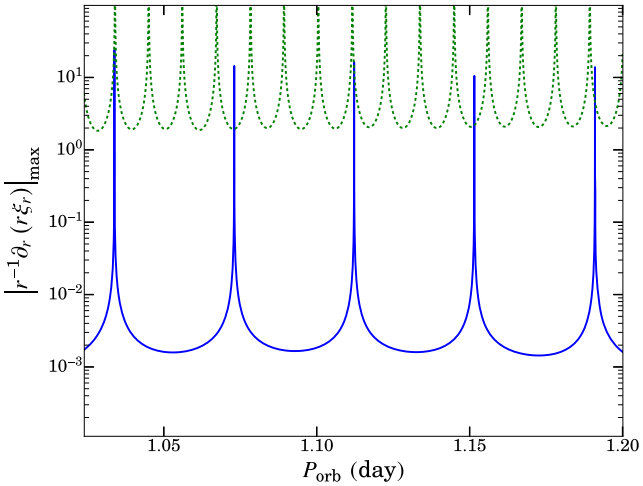

Figure 4. The breaking criterion in linear theory as a function of orbital period $P_{\rm orb} = 4\pi/\omega$. The wave can sufficiently overturn stratification and break when $|r^{-1}\partial_r (r\xi_r)|_{\max} > 1$. Curves are displayed for our main-sequence model A (solid blue) and subgiant model B (dotted green).

moment of inertia of the synchronously rotating core is

$$I_{\rm spin} = m_{\rm b} a^2 \left[\left(1 + \frac{\Delta t (1-2\eta)\tau}{m_{\rm b}\sqrt{G M_* a}} \right)^{\frac{1}{1-2\eta}} - 1 \right], \tag{14}$$

where the τ and a refer to present day values. In the following, we adopt the form of the torque in equation (7) ($\eta = -10$) and use model B to estimate relevant stellar quantities. For model B, the time between the best-fitting model and the disappearance of a convective core is $6 \gtrsim \Delta t \gtrsim 3$ Myr. But because the precursor to model B that has not yet lost its convective core still manages to fit the observables well, the actual Δt could be made arbitrarily small and it's better to take $6 \gtrsim \Delta t \gtrsim 0$ Myr . On the one hand, we could be seeing this system 100 yr after the convective core disappeared, in which case the core has not been spun-up significantly, but probabilistically it's most likely we are seeing this system on the order of millions of years after the convective core disappeared. Even models 10–100 Myr after the core disappeared do not fit the observables terribly, but using one of these values does not change the radial extent of the spun-up core due to the steep dependence of τ on a. This fact is shown in Fig. 5 where we scale the upper abscissa with the value of the radius of the synchronously rotating core $R_{\rm spin}$ to the corresponding Δt on the lower abscissa. This insensitivity of $R_{\rm spin}$ on Δt provides a potentially testable prediction of the dynamical tide explanation – if WASP-12b's decay is an effect of the dynamical tide, the innermost $\approx 0.2 R_\odot$ of WASP-12 itself should be rapidly rotating.

Because the linear rotational frequency of this core $\nu_{\rm rot} = 66\,\mu$Hz is significantly less than the linear eigenfrequencies of our subgiant model, the rotational splittings can be estimated in a perturbative manner as in Aerts, Christensen-Dalsgaard & Kurtz (2010). For azimuthal order m, the splittings $\delta\nu$ can be written as

$$\delta\nu = m \int_0^{R_*} K_{nl}(r)\nu_{\rm rot}(r)\,{\rm d}r, \tag{15}$$

where K_{nl} is the unnormalized rotational kernel for radial order n, angular order l,

$$K_{nl} \equiv \frac{\int_0^{R_*} \left[\xi_r^2 + l(l+1)\xi_h^2 - 2\xi_r\xi_h - \xi_h^2\right] \rho r^2 {\rm d}r}{\int_0^{R_*} \left[\xi_r^2 + l(l+1)\xi_h^2\right] \rho r^2 {\rm d}r}. \tag{16}$$

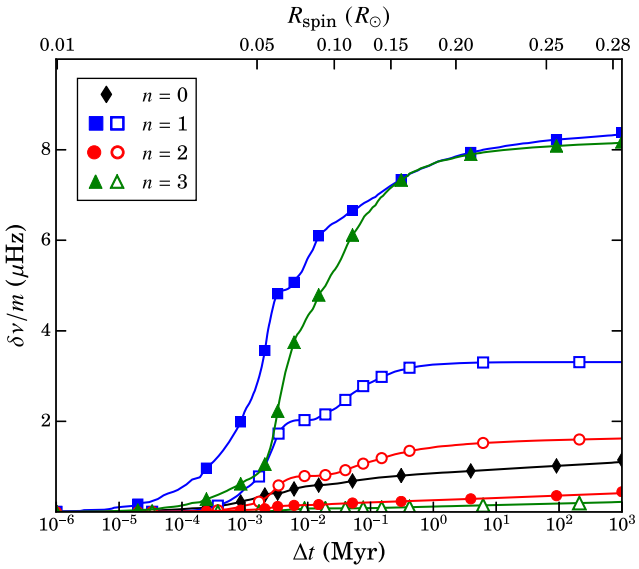

Figure 5. Low-order frequency splittings of model B due to a synchronously spinning stellar core versus its radius $R_{\rm spin}$, or equivalently, versus the duration Δt of the tidal torque. Marker shape denotes the radial order for a mode. Shaded markers correspond to $l = 2$ modes, while empty markers denote $l = 1$ mode.

We present several of these low-order rotational splittings in Fig. 5 as a function of the size of the spinning core, and find that they are on the order of a few μHz. Compare this to the corresponding rotational splittings in a model rotating uniformly at the measured $v \sin i_* = 1.6$ km s^{-1}; though the splittings would be enhanced by non-zero contributions from the entire star, ultimately they would remain orders of magnitude smaller owing to a much lower $\nu_{\rm rot}$.

5 DISCUSSION

We have seen that the apparent period change ($\dot{P}$) observed in the transits of WASP-12b cannot easily be explained as secular orbital decay. Standard mechanisms of tidal dissipation are too slow, unless the orbit happens to be close to resonance with a global g-mode. We have estimated the probability for this to be quite small.

The leading alternative explanation for the anomalous transit times is that the planetary orbit is slightly eccentric, $e \approx 2 \times 10^{-3}$. In this interpretation, the true orbital period is constant, but the transit times depart slightly from a linear ephemeris due to precession of periastron at a rate $\dot{\omega} \approx 26^\circ$ yr^{-1} (Maciejewski et al. 2016; Patra et al. 2017). The latter authors estimate that for a reasonable tidal quality factor of the planet itself, $Q_{\rm p} \leq 10^6$, any primordial eccentricity would have decayed to $e < 10^{-3}$ after a few million years, whereas the system age appears to be > 1 Gyr. Therefore, the eccentricity would have to be recently excited or continually forced.

We now briefly examine mechanisms for forcing the eccentricity or modulating the period of the orbit via changes in host star or third bodies.

In the following, unless otherwise noted, we take $M_* = 1.4\,M_\odot$, which is slightly higher than any of the values in Table 2. Therefore $R_* = 1.64\,R_\odot$ based on the mean density adopted in Table 1. With Southworth (2012)'s result that $R_{\rm b}/R_* \approx 0.1159 \pm 0.0033$, we then have $R_{\rm b} \approx 1.89 R_{\rm J}$ for the planetary radius. Both radii would scale $\propto M_*^{1/3}$ to other assumed values of the stellar mass. Adopting the radial velocity amplitude $K = 221.9 \pm 3.1$ m s^{-1} from Knutson et al. (2014) and the inclination $I = (83^\circ \pm 0.^\circ 5)$ from Maciejewski et al.

(2013), and since $m_b(M_* + m_b)^{-2/3} = K_* \sec I (P/2\pi G)^{1/3}$, we then have $m_b = 1.41\ M_J$; this scales approximately as $M_*^{1/3}$. Finally, the semimajor axis becomes $a = (P/2\pi)^{2/3}[G(M_* + m_b)]^{1/3} \approx 0.02322$ au.

5.1 Eccentricity from convection

Phinney (1992) proposed that the small measured eccentricities of binary millisecond pulsars with white dwarf companions can be explained by potential fluctuations associated with convection in the envelope of the companion when on the giant or asymptotic giant branch. With few exceptions, the orbits of subsequently discovered binary millisecond pulsars have conformed well to the predictions of this model (Lorimer 2008).

Adapted to the WASP-12 system, so that the reduced mass $\mu \approx 1.4\ M_J$, Phinney's equation (7.33) reads

$$\langle e^2 \rangle^{1/2} \approx 2 \times 10^{-5} \left(\frac{L_* R_{env}}{5\,L_\odot R_\odot} \frac{1.4\,M_\odot}{M_*} \right)^{1/3} \left(\frac{M_{env}}{0.0004\,M_\odot} \right)^{1/6}, \quad (17)$$

in which $R_{env} \approx 1.4\,R_\odot$ is the radius at the base of the outer convection zone in our preferred model for WASP-12. M_{env}, the mass of that zone, is sensitive to the effective temperature, metallicity, and evolutionary state of the star, but in view of the sixth root, no plausible value of M_{env} could make up the two orders of magnitude by which the rms eccentricity predicted by equation (17) falls short of the value required to explain the quadratic term in the transit ephemeris. Furthermore, as Phinney remarks, his equation (7.33) probably overestimates the eccentricity expected when the turnover time of the largest convective eddies exceeds the tidal period, as occurs in WASP-12 by at least one order of magnitude.

5.2 The Applegate effect

Applegate & Patterson (1987) and Applegate (1992) suggested that long-term modulations observed in the eclipse times of some close stellar binaries, including V471 Tau and Algol, are caused by slow changes in the quadrupole moment of one or both stars induced by their magnetic cycles. In the later version of this idea, the magnetic stress is not large enough to distort the equilibrium shape of the star directly, but rather slowly redistributes angular momentum within the star(s), leading to changes in the rotationally induced quadrupole. Because the changes are slow, they would not excite the eccentricity of the orbit, but the quadrupole contributes to the central force between the stars and hence to the orbital period itself. Watson & Marsh (2010, hereafter WM10) have scaled Applegate (1992)'s model to several exoplanet systems. For WASP-12b, they estimate that the anomaly in the transit time ($O - C$, observed minus calculated) could be as much as 42 $(T/50\,\mathrm{yr})^{3/2}$ s, where T is the period on which the dynamo modulates the internal differential rotation. This last could be the same as the period of the magnetic dipole, or half that, depending on the type of dynamo.

WM10's predicted variation is not a great deal smaller than the ∼2-min departure from a linear transit ephemeris found by Patra et al. (2017). It depends on several uncertain parameters besides the dynamo period T, so one ought to consider whether the uncertainties in these parameters might allow the Applegate effect to explain the WASP-12 data. The relevant parameters are the rotation period of the star, for which WM10 take $P_{rot} = 36$ d, the fractional mass of the convection zone, for which they take $M_{env}/M_* = 0.1$, and the portion of the mean luminosity that is converted to mechanical form to change the differential rotation. For the latter they take $\Delta L = 0.1\ L$; this seems large, but perhaps not in direct conflict with observations because, as they point out, the luminosity variation at the photosphere could be much smaller due to the thermal inertia of the convection zone (i.e. the ratio of its total thermal energy to the luminosity of the star; this is about 300 yr for WASP-12). WM10's equations imply that the transit time anomalies scale with these parameters as follows:

$$(O - C)_{max} \propto T^{3/2} P_{rot}^{-1} \left(\frac{M_{env}}{M_*} \right)^{1/2} (\Delta L)^{1/2}. \quad (18)$$

The mass of the convective envelope of WASP-12 is probably $\lesssim 10^{-3}\ M_*$, as remarked above; following equation (18), this would reduce the predicted $O - C$ by an order of magnitude. On the other hand, the rotation period may be rather less than the assumed value if the star is viewed near pole on, as Rossiter–McLaughlin measurements suggest (Albrecht et al. 2012). The median rotation period for main-sequence F8 stars[3] is ≈8 d (Nielsen et al. 2013). Since dynamo periods appear to correlate positively with stellar rotation periods (Saar & Brandenburg 1999; Böhm-Vitense 2007), however, the positive scaling with T seems likely to overwhelm the negative scaling with P_{rot} in equation (18).

If WM10's scalings are applied to the Sun, they predict a variation $\Delta J_2 \gtrsim 5 \times 10^{-8}$ in its rotationally induced dimensionless quadrupole moment over the dynamo cycle. The internal differential rotation of the Sun has been directly constrained by helioseismology, and for a significant fraction of a cycle. Antia, Chitre & Gough (2008) have used these data to estimate that $\langle J_2 \rangle_\odot = 2.2 \pm 0.01 \times 10^{-7}$, and the variation over a 9-yr period to be $\lesssim 1 \times 10^{-10}$, i.e. several orders of magnitude smaller than WM10's assumptions would predict.

For these reasons (i.e. both our estimates of the actual parameters of WASP-12, as well as comparison with heliosesimological inferences for the Sun), it is unlikely that the Applegate effect explains the transit time anomalies of WASP-12b.

5.3 Bow shock

Ultraviolet absorption is seen just before each transit of WASP-12b and has been interpreted as evidence for mass loss from the planet through its inner Lagrange point (Fossati et al. 2010a). Alternatively, this could be the signature of a bow shock ahead of the planet encountering a wind from the star (Lai, Helling & van den Heuvel 2010; Vidotto, Jardine & Helling 2010). Such a shock would exert a drag on WASP-12b's orbit. As shown here, however, an improbably dense wind would be required to explain the observed $\dot{P}$.

The torque exerted on the planet by the shock is $C_D \pi R_b^2 \rho_w (v_b^2 + v_w^2)^{1/2} v_b a$, in which C_D is a factor of order unity (the drag coefficient), ρ_w the pre-shock density of the wind, v_w the wind velocity, $R_b \approx 1.9\ R_J$ the radius of the planet, and $v_b \approx (GM_*/a)^{1/2}$ the orbital velocity. The decay time-scale is then

$$\frac{P}{\dot{P}} = \frac{m_b}{3\pi C_D R_b^2 \rho_w (v_b^2 + v_w^2)^{1/2}} \approx 4 \times 10^{12}\ \mathrm{yr}. \quad (19)$$

For the numerical estimate, we have taken $C_D = 0.3$, and $\rho_w = 2 \times 10^{-18}\ \mathrm{g\,cm^{-3}}$ (i.e. $n_H = 1.5 \times 10^6\ \mathrm{cm^{-3}}$); the latter follows Vidotto et al. (2010) and implies a stellar mass-loss rate of $10^{-12.3}(v_{wind}/100\ \mathrm{km\,s^{-1}})\ M_\odot\ \mathrm{yr^{-1}}$. In order to explain the apparent decay rate ($P/\dot{P} \approx 3$ Myr), the wind density would have to increase

[3]Hebb et al. (2009) classify WASP-12 as F9V.

some six orders of magnitude, making the mass-loss time-scale of the star $\lesssim$10 Myr. This is unreasonable as the star is probably older than 1 Gyr.

5.4 Kozai–Lidov oscillations

We consider the possibility that a non-transiting third body in the system continuously excites a small eccentricity in the orbit of WASP-12b so that, as suggested by Maciejewski et al. (2016), the transit time anomalies result from apsidal precession of the slightly elliptical orbit.

Apsidal precession itself imposes a lower bound on the perturbations that such a hypothetical companion must exert to excite WASP-12b's eccentricity. Let the companion have mass m_c, semi-major axis a_c, and orbital eccentricity e_c, and let $\{m_b, a_b, e_b\}$ be those of WASP-12b itself. By a standard calculation in secular perturbation theory, one can show that if $e_b \ll 1$ initially, then e_b will grow by the Kozai–Lidov mechanism (hereafter KLM) only if

$$\frac{m_c}{a_c^3(1-e_c^2)^{3/2}} > \frac{10}{3} k_{2b} \frac{M_*^2 R_b^5}{m_b a_b^8}, \tag{20}$$

in which R_b is the radius of WASP-12b and k_{2b} its Love number, these two quantities being important for the apsidal precession rate. The inequality (equation 20) assumes that the orbital planes of m_c and m_b are orthogonal, which maximizes the efficiency of the KLM. We are also assuming $a_c > a_b$, i.e. the third body's orbit is exterior to that of WASP-12b. The orbits should not cross, whence $a_c(1-e_c) > a_b$, and therefore $a_c(1-e_c^2)^{1/2} > \sqrt{a_b a_c}$. With $k_{2b} \approx 0.6$ (Wahl, Hubbard & Militzer 2016), the lower bound on the companion's mass for the KLM becomes

$$m_c > 77 \left(\frac{a_c}{a_b}\right)^{3/2} \mathrm{M}_\oplus. \tag{21}$$

An upper bound on m_c follows from the published radial velocity data (Hebb et al. 2009; Husnoo et al. 2011; Albrecht et al. 2012; Bonomo et al. 2017). After subtraction of the WASP 12b signal[4] and correction for the nominal measurement errors, these data have variance $\approx (9\,\mathrm{m\,s^{-1}})^2$. The radial velocity signal of the hypothetical WASP-12c should be no larger than this. Therefore,

$$m_c < 18\, f^{-1/2} \left(\frac{a_c}{a_b}\right)^{1/2} \mathrm{M}_\oplus, \tag{22}$$

with f being a geometrical factor that determines the mean square projection of the orbital velocity on to the line of sight:

$$f(e_c, \omega_c, I_c) = \frac{\sin^2\omega_c + \sqrt{1-e_c^2}\,\cos^2\omega_c}{1+\sqrt{1-e_c^2}} \sin^2 I_c\,. \tag{23}$$

In order that the KLM operate, the relative inclination of the two planetary orbits must be greater than $\sin^{-1}\sqrt{2/5} \approx 39.^\circ2$, so

$$\cos I_c \cos I_b + \sin I_c \sin I_b \cos(\Omega_c - \Omega_b) < \sqrt{3/5},$$

with $\Omega_{b,c}$ being the longitudes of the ascending nodes. Since the inclination of WASP 12b is $I_b \approx (83^\circ \pm 0.^\circ5)$ (Maciejewski et al. 2013), the above constraint is compatible with $I_c \approx 0$, and of course also with any eccentricity e_c or argument of periastron ω_c. So the factor f could be arbitrarily small. The two inequalities (21) and (22) could therefore both be satisfied by an exterior perturber ($a_c > a_b$), although this becomes less probable as the separation between the orbits increases because of the different scalings with a_c/a_b. Furthermore, equations (22) and (23) suppose that the radial velocity is measured continuously, whereas in fact it is sampled somewhat sparsely and irregularly: nearly half of the ~90 measurements were made by Albrecht et al. (2012) in a single night. If WASP 12c's orbit were highly eccentric, and thus hovering usually near apastron, its full radial velocity amplitude might not be sampled.

We have not systematically investigated the probability that both of the mutually antagonistic bounds (21) and (22) could be satisfied. Nevertheless, the Kozai–Lidov mechanism does not seem to provide a natural explanation for the quasi-secular transit time anomalies of WASP 12b. The hypothesis is attractive only in comparison to all of the other possibilities that we have investigated.

5.5 Resonance

We have considered the possibility that the orbital variations of WASP 12b are caused by resonant interactions with an unseen planet. We focus on mean motion resonances.

Suppose first a 1:1 resonance, in other words, a small Trojan planet librating around the stable Lagrange points of the WASP-12 + WASP-12b system.[5] The inferred amplitude of the period variation is $29 \pm 3\,\mathrm{ms\,yr^{-1}}$ (Patra et al. 2017), amounting to $\Delta \ln P \approx 3 \times 10^{-6}$ over the 9 yr that transits have been monitored. We estimate that a roughly lunar mass in a 'horseshoe' 1:1 resonant libration could modulate WASP 12b's period at this amplitude. This would easily satisfy the limit $m_c < 34\,\mathrm{M}_\oplus$ on Trojan companions to WASP-12b found by Lillo-Box et al. (2018), who based their analysis on archival radial velocities. The difficulty, however, is in the period of the modulation. It is well known that small-amplitude librations around the Lagrange points in the coplanar restricted three-body problem have period $P_{\rm lib} = P_{\rm orb} \times 2(1+q)/\sqrt{27q}$, where $P_{\rm orb}$ is the orbital period of the massive bodies and $q < 0.04$ is their mass ratio. In the present case where $P_{\rm orb} = 1.09$ d and $q \approx 10^{-3}$, $P_{\rm lib} \approx 13$ d. A large-amplitude libration can have a somewhat longer period than this, but not by more than a factor of ~2 unless very close to the separatrix between libration and circulation, as we have convinced ourselves by numerical experiments. Such a $P_{\rm lib}$ is far too short to mistaken for a secular trend over 9 yr unless severely aliased, which seems unlikely in view of the density of transit observations (see the tabulation in Patra et al. 2017).

We have also examined first-order mean motion resonances $P_c : P_b \approx (j+1) : j$, with $j \geq 1$ an integer. Our analysis is restricted to coplanar, near-circular cases, but the main conclusions would probably be similar even for strongly misaligned orbits. The unseen body WASP-12c is presumed to be much less massive than WASP-12b.

Close to such a resonance, the jth azimuthal harmonic of the potential of the orbit of b directly forces the eccentricity of c's orbit (e_c), and the $(j+1)$th harmonic of c forces e_b. In the first case, or 'exterior' resonance, e_b is neglected to leading order, while e_c is neglected for the interior resonance (e.g. Murray & Dermott 2000). The forced eccentricities depend not only on the masses m_c and m_b but also on the distances from exact resonance; these differ because of the unforced apsidal precession rates of the two planets. As already noted in Section 5.4, the apsidal precession of b is dominated by its tidal distortion: we estimate $\varpi_{b0} \approx 3.7 \times 10^{-4} n_b$,

[4] We subtract an optimally scaled multiple of the photometric ephemeris of Patra et al. (2017), including their secular period derivative $\dot{P} = (0.92 \pm 0.01) \times 10^{-9}$. Thus this limit applies to companions with periods less than the span of the data, ~7 yr.

[5] We thank Scott Tremaine for suggesting that we look into this.

with $n_b = 2\pi P_b^{-1}$ being its mean motion. If c is a smaller body such as a superearth, its apsidal motion is dominated by the axisymmetric potential of b's orbit. Near the 2:1 resonances, we estimate that $\dot{\varpi}_{c0} \approx 3.73 \times 10^{-4} n_b$. Because of the coincidence that $\dot{\varpi}_b \approx \dot{\varpi}_b$, the slow frequencies that measure the distance from resonance, namely $\nu_b \equiv j n_b - (j+1) n_c + \dot{\varpi}_{b0}$ and $\nu_c \equiv j n_b - (j+1) n_c + \dot{\varpi}_{c0}$ will usually be nearly equal, at least for the 2:1 resonances ($j = 1$).

The damping rate of eccentricity due to tidal dissipation in planet p is (Goldreich & Soter 1966)

$$\gamma_p \equiv -\left(\frac{\mathrm{d}\ln e}{\mathrm{d}t}\right)_{\rm tide} = \frac{63}{4Q'_p}\frac{M_*}{m_p}\left(\frac{R_p}{a_p}\right)^5 n_p, \tag{24}$$

where $Q'_p \equiv 3Q_p/2k_{2,p}$ is the tidal quality factor of the planet corrected for its Love number. On short time-scales $\sim \nu^{-1}$, an equilibrium holds between forcing and damping. Secularly however, at second order in eccentricity and first order in the damping rate (equation 24), there is a transfer of orbital energy and angular momentum between planets. The transfer is always outward, i.e. from b to c, but in the proportion $\Delta E = n_c \Delta J$ for the interior resonance (where the orbit of c is approximated as circular), and $\Delta E = n_b \Delta J$ for the exterior resonance (where Δe_b is neglected). The rate of transfer of angular momentum is related to the tidal dissipation rates $\dot{\mathcal{E}}_{b,c} > 0$ by

$$\frac{\mathrm{d}J_c}{\mathrm{d}t} = -\frac{\mathrm{d}J_b}{\mathrm{d}t} = \frac{\dot{\mathcal{E}}_b + \dot{\mathcal{E}}_c}{n_b - n_c}. \tag{25}$$

The effect of this torque is to increase the slow frequencies ν_b and ν_c, and hence to increase the distance from resonance if these frequencies are already positive.

If $m_c \sim \mathrm{M}_\oplus$ and $Q'_c \lesssim 10^{-4} Q'_b$, we estimate that $\dot{\mathcal{E}}_b > \dot{\mathcal{E}}_c$ by a factor of at least a few at the first few mean motion resonances ($j \lesssim 5$). Balancing forcing and dissipation,

$$\dot{\mathcal{E}}_b = \gamma_b m_b (n_b a_b e_b)^2 \approx \frac{\gamma_b m_b A_b^2}{\nu_b^2 + \gamma_b^2}, \tag{26}$$

in which e_b is the forced eccentricity of body b, and

$$A_b = \frac{G m_c}{2 a_b a_c}\left[\frac{\mathrm{d}}{\mathrm{d}\ln\alpha} b_{1/2}^{(j+1)}(\alpha) + 2j b_{1/2}^{(j+1)}(\alpha)\right]_{\alpha = a_b/a_c}, \tag{27}$$

in terms of the usual Laplace coefficients. (These equations also determine $\dot{\mathcal{E}}_c$ if all subscripts 'b' and 'c' are interchanged and $j \to j - 1$.) Presuming that $m_c \ll m_b$, the increase in ν due to the torque (25) is dominated by the change in the mean motion of c: $\dot{\nu} \approx -(j+1)\dot{n}_c$. We focus on the interior resonance where e_b is excited and hence take c's orbit to remain circular, $n_c \propto J_c^{-3}$. Also $\dot{J}_c \approx -(j+1)\dot{\mathcal{E}}_b/n_b$ from equation (25) with $\dot{\mathcal{E}}_c \ll \dot{\mathcal{E}}_b$.

For definiteness, let us focus on the 2:1 resonance, $j = 1$, so that the detunings $\nu_c \approx \nu_b \equiv \nu$ by the numerical coincidence noted above. In the relevant regime where $n_c \gg \nu \gg \gamma$, equations (26) and (27) imply that $\mathrm{d}\nu/\mathrm{d}t \propto \nu^{-2}$. Integrating this relation with the constants included yields

$$\nu \approx 0.036\left(\frac{10^6}{Q'_b}\frac{m_c}{\mathrm{M}_\oplus}\frac{T}{\mathrm{Gyr}}\right)^{1/3} n_b, \tag{28}$$

in which T is the time elapsed since exact resonance.

The quantities in parentheses in equation (28) are uncertain, but because of the cube root, it is unlikely that the fractional distance from resonance (ν/n_b) is much less than 10^{-2}. Now at a $(j+1)$:j resonance, the combination $(j+1)n_c - j n_b$ is the *forced* apsidal precession rate, $\dot{\varpi}_b$. Therefore $\nu = \dot{\varpi}_{b0} - \dot{\varpi}_b$. Since we have previously estimated that $\dot{\varpi}_{b0} \approx 4 \times 10^{-4} n_b$, it follows from equation (28) that $\dot{\varpi}_b < 0$, with a period $\sim (0.036)^{-1} \times P_b \approx 30$ d. There are thus at least two objections to mean motion resonances as a mechanism for sustaining $e_b \approx 2 \times 10^{-3}$. First, at the distance ν from resonance that we have just estimated, the required mass of the hypothetical planet c is comparable to that of WASP-12b itself. A smaller mass would suffice closer to resonance ($m_c \propto \nu$ at fixed e_b), but tidal dissipation would then double the distance from resonance in much less than the system's current age. Secondly, the period of the forced apsidal precession is much too rapid to explain the observed quasi-secular $\dot{P}$ unless, again, the system was improbably close to exact resonance. These difficulties are even more severe for $j > 1$.

6 SUMMARY

We have revisited the possible causes of WASP-12b's departure from a linear ephemeris. Either the orbit is decaying, or some dynamical perturbation maintains a small eccentricity and the apsides precess on some period longer than a decade. We have considered various perturbations induced by unseen third bodies or distortions of the star WASP-12 itself, but none is consistent with all of the observational constraints, at least not without fine tuning.

The conclusion therefore seems inescapable that the orbit is indeed decaying, presumably because of tidal dissipation in the star. Indeed, the dynamical tide – computed for a circular orbit and a negligibly rotating star – naturally yields an orbital lifetime comparable to what is inferred from transit timing. But this requires that the star has evolved on to the subgiant branch and lost its convective core, as Weinberg et al. (2017) have suggested. In that case, the g-modes excited at the base of WASP-12's thin surface convection zone might be just strong enough to damp non-linearly in the core, which would broaden the g-mode resonances so that they overlapped. If WASP-12 were still on the main sequence and still had its convective core, the resonances would be very sharp, and the orbit would have to be implausibly close to resonance to explain the current rate of orbital evolution. Alternatively, if the star had a *rapidly rotating* core, with a rotation period as short or shorter than the period of the orbit, then the tidally excited g-modes would be absorbed at the critical (corotation) layer (Barker & Ogilvie 2010); the torque applied by absorption of the ingoing waves would then maintain the rapid rotation of the layer and presumably of the core beneath it. This begs the question how the core could have started out with such rapid rotation, however. Moreover, unlike the subgiant hypothesis, it does not naturally explain why the decay time-scale is so much shorter than the age of the star.

The observational constraints on WASP-12 itself, when fit to theoretical models for its structure made with the MESA code, favour a main-sequence star rather than a subgiant, and even the main-sequence models prefer $T_{\rm eff} > 6300$ K, in line with Collins et al. (2017) but higher than the weighted average of older measurements (Table 1). Further accurate measurements of $T_{\rm eff}$, [Fe/H], and A_V for this star could be helpful, although in view of the theoretical uncertainties with regard to α and other mixing parameters, perhaps only an asteroseismic detection of core rotation would be decisive.

ACKNOWLEDGEMENTS

We thank Josh Winn for introducing us to this problem and for much helpful advice and conversation, and the referee Adrian Barker for constructive criticism. We also greatly benefitted from insightful

discussions with Keivan Stassun, Scott Gaudi, and Nevin Weinberg concerning the observational constraints on WASP-12.

This work has made use of data from the European Space Agency (ESA) mission *Gaia* (https://www.cosmos.esa.int/gaia), processed by the *Gaia* Data Processing and Analysis Consortium (DPAC; https://www.cosmos.esa.int/web/gaia/dpac/consortium). Funding for the DPAC has been provided by national institutions, in particular the institutions participating in the *Gaia* Multilateral Agreement.

REFERENCES

Aerts C., Christensen-Dalsgaard J., Kurtz D. W., 2010, Asteroseismology. Springer, New York
Albrecht S. et al., 2012, ApJ, 757, 18
Allende Prieto C., Asplund M., García López R. J., Lambert D. L., 2002, ApJ, 567, 544
Antia H. M., Chitre S. M., Gough D. O., 2008, A&A, 477, 657
Applegate J. H., 1992, ApJ, 385, 621
Applegate J. H., Patterson J., 1987, ApJ, 322, L99
Asplund M., Grevesse N., Sauval A. J., Scott P., 2009, ARA&A, 47, 481
Aufdenberg J. P., Ludwig H.-G., Kervella P., 2005, ApJ, 633, 424
Barker A. J., Ogilvie G. I., 2010, MNRAS, 404, 1849
Bechter E. B. et al., 2014, ApJ, 788, 2
Bedding T. R. et al., 2010, ApJ, 713, 935
Bergfors C. et al., 2013, MNRAS, 428, 182
Böhm-Vitense E., 2007, ApJ, 657, 486
Bond H. E. et al., 2015, ApJ, 813, 106
Bonomo A. S. et al., 2017, A&A, 602, A107
Chernov S. V., Ivanov P. B., Papaloizou J. C. B., 2017, MNRAS, 470, 2054
Choi J., Dotter A., Conroy C., Cantiello M., Paxton B., Johnson B. D., 2016, ApJ, 823, 102
Collins K. A., Kielkopf J. F., Stassun K. G., 2017, AJ, 153, 78
Fossati L. et al., 2010a, ApJ, 714, L222
Fossati L. et al., 2010b, ApJ, 720, 872
Gaia Collaboration et al., 2016, A&A, 595, A1
Gaia Collaboration et al., 2018, A&A, 616, A1
Goldreich P., Nicholson P. D., 1977, Icarus, 30, 301
Goldreich P., Soter S., 1966, Icarus, 5, 375
Goodman J., Dickson E. S., 1998, ApJ, 507, 938
Green G. M. et al., 2018, MNRAS, 478, 651
Hebb L. et al., 2009, ApJ, 693, 1920
Husnoo N. et al., 2011, MNRAS, 413, 2500
Husnoo N., Pont F., Mazeh T., Fabrycky D., Hébrard G., Bouchy F., Shporer A., 2012, MNRAS, 422, 3151
Jerzykiewicz M., Molenda-Zakowicz J., 2000, Acta Astron., 50, 369
Knutson H. A. et al., 2014, ApJ, 785, 126
Kushnir D., Zaldarriaga M., Kollmeier J. A., Waldman R., 2017, MNRAS, 467, 2146
Lai D., Helling C., van den Heuvel E. P. J., 2010, ApJ, 721, 923
Levrard B., Winisdoerffer C., Chabrier G., 2009, ApJ, 692, L9
Lillo-Box J., Barrado D., Figueira P., Leleu A., Santos N. C., Correia A. C. M., Robutel P., Faria J. P., 2018, A&A, 609, A96
Lorimer D. R., 2008, Living Rev. Relativ., 11, 8
Maciejewski G. et al., 2013, A&A, 551, A108
Maciejewski G. et al., 2016, A&A, 588, L6
Mortier A., Santos N. C., Sousa S. G., Fernandes J. M., Adibekyan V. Z., Delgado Mena E., Montalto M., Israelian G., 2013, A&A, 558, A106
Murray C. D., Dermott S. F., 2000, Solar System Dynamics. Cambridge Univ. Press, Cambridge
Nielsen M. B., Gizon L., Schunker H., Karoff C., 2013, A&A, 557, L10
Ogilvie G. I., Lesur G., 2012, MNRAS, 422, 1975
Patra K. C., Winn J. N., Holman M. J., Yu L., Deming D., Dai F., 2017, AJ, 154, 4
Paxton B., Bildsten L., Dotter A., Herwig F., Lesaffre P., Timmes F., 2011, ApJS, 192, 3
Paxton B. et al., 2013, ApJS, 208, 4
Paxton B. et al., 2015, ApJS, 220, 15
Paxton B. et al., 2018, ApJS, 234, 34
Penev K., Sasselov D., Robinson F., Demarque P., 2007, ApJ, 655, 1166
Penev K. et al., 2016, AJ, 152, 127
Phinney E. S., 1992, Philos. Trans. R. Soc. Lond. Ser. A, 341, 39
Remus F., Mathis S., Zahn J.-P., 2012, A&A, 544, A132
Saar S. H., Brandenburg A., 1999, ApJ, 524, 295
Southworth J., 2012, MNRAS, 426, 1291
Stassun K. G., Torres G., 2018, ApJ, 862, 61
Stassun K. G., Collins K. A., Gaudi B. S., 2017, AJ, 153, 136
Terquem C., Papaloizou J. C. B., Nelson R. P., Lin D. N. C., 1998, ApJ, 502, 788
Torres G., Fischer D. A., Sozzetti A., Buchhave L. A., Winn J. N., Holman M. J., Carter J. A., 2012, ApJ, 757, 161
van Saders J. L., Pinsonneault M. H., 2012, ApJ, 746, 16
Vidotto A. A., Jardine M., Helling C., 2010, ApJ, 722, L168
Wahl S. M., Hubbard W. B., Militzer B., 2016, ApJ, 831, 14
Watson C. A., Marsh T. R., 2010, MNRAS, 405, 2037 (WM10)
Weinberg N. N., Sun M., Arras P., Essick R., 2017, ApJ, 849, L11
Zahn J. P., 1966, Ann. d'Astrophys., 29, 489
Zahn J.-P., 1977, A&A, 57, 383
Zahn J.-P., 2013, in Souchay J., Mathis S., Tokieda T., eds, Lecture Notes in Physics, Vol. 861, Tides in Astronomy and Astrophysics. Springer-Verlag, Berlin, p. 301

This paper has been typeset from a TEX/LATEX file prepared by the author.